



ELSEVIER

Journal of Nuclear Materials 258–263 (1998) 335–338

Journal of
nuclear
materials

Influence of materials choice on occupational radiation exposure in ITER

C.B.A. Forty ^{a,*}, J.D. Firth ^a, G.J. Butterworth ^b

^a UKAEA Fusion, Culham Science Centre, Abingdon, Oxfordshire, OX14 3DB, UK

^b Butterworth and Associates, West Ilsley, Newbury, Berkshire, RG20 7AL, UK

Abstract

In fission reactor plant, the radiation doses associated with inspection and maintenance of the primary cooling circuit account for a substantial fraction of the collective occupational radiation exposure (ORE). Similarly, it is anticipated that much of the ORE occurring during normal operation of ITER will arise from active deposits in the cooling loop. Using a number of calculation steps ranging from neutron activation analysis, mobilisation and transport modelling and Monte Carlo simulation, estimates for the gamma photon flux and radiation dose fields around a typical 'hot-leg' cooling pipe have been made taking SS316, OPTSTAB, MANET-II and F-82H steels as alternative candidate loop materials. © 1998 UKAEA. Published by Elsevier Science B.V. All rights reserved.

1. Introduction

According to present designs [1], the fusion power core of ITER will be cooled by 20 pressurised water loops, of which 10 are dedicated to cooling first wall and blanket modules. Each first wall/blanket (FW/BL) loop can be assumed to consist of the following essential features, shown schematically in Fig. 1: a portion of the first wall/shielding blanket containing a large number of small diameter pipes, various manifolds, a single 'hot-leg' pipe, a heat exchanger, a 'cold-leg' return, a circulating pump and a chemical volume control system (CVCS) employing filters and ion exchangers.

The interaction of neutrons with the first wall, divertor and blanket structures results in their activation. Since these structures lie well within the biological shield, they pose no direct radiation hazard to operating personnel. Activated material can, however, be released into the coolant from in-core pipe surfaces through a number of processes, notably corrosion, erosion, dissolution, dynamic recoil sputtering from near surface pipe atoms and diffusion. Inactive material liberated from coolant loop surfaces outside the core can also become

activated during repeated passage through the core. In the present context the material products of these processes can simply be termed: "activated corrosion products" (ACPs).

While a fraction of the mobilised material is captured in the CVCS, the bulk is deposited onto surfaces in other regions of the cooling loop. Thus those parts of the coolant circuit outside the biological shield, in particular the main 'hot-leg' pipes, heat exchangers, CVCS and pumps, can become internally contaminated with active species. Since access to these components is needed for periodic inspection and maintenance, workers undertaking these tasks will be exposed to γ radiation from the wall deposits. Earlier work [2] suggests that this exposure route may be a major contributor to occupational radiation exposure (ORE) in ITER, and it is therefore an important topic for study. In the present work, calculations have been performed to estimate the γ fluxes and radiation fields expected around a typical hot-leg pipe in one of the main ITER FW/BL cooling loops. For comparison, four different steels have been considered as the primary coolant loop pipe material. These include the standard ITER grade SS316 austenitic stainless steel and a low activation austenitic analogue, OPTSTAB. Two martensitic steels are also examined. These are the European MANET-II steel and a Japanese low activation martensitic, F-82H.

* Corresponding author. Tel.: +44 1235 463232; fax: +44 1235 463435; e-mail: cleve.forty@ukaea.org.uk.

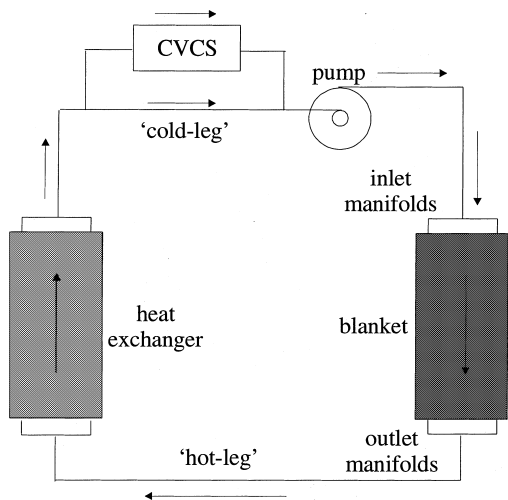


Fig. 1. Single ITER FW/BL cooling loop showing the main equipment.

2. Method of calculation

The sequence of steps in the calculation involves the use of a number of data libraries and codes as is illustrated schematically in Fig. 2.

2.1. Steel activation analyses

As a necessary simplification it is assumed that the entire coolant circuit is made from the selected material. The assumed starting compositions of the four steels chosen for study are presented in Table 1.

Earlier work [3] has demonstrated that the pulsed operation schedule envisaged for the ITER extended performance phase (EPP) can be represented by a simplified model in which the initial short-pulse phase is treated as a continuous operation at a time-averaged wall loading, while the final phase comprising 84 cycles of 1 h power-on, 1 h power-off operation at the nominal wall loading of 3 MW m⁻² is modelled in more detail.

With the above material compositions and irradiation regime, and taking an average blanket neutron flux of 2.57 × 10¹⁷ n m⁻² s⁻¹, the radionuclide inventory pertaining to the blanket tubes in ITER has been calculated using the neutron activation code FISPACT-97 [4] in conjunction with the EAF-97 [5,6] nuclear data libraries. The entire shutdown inventory was utilised (a conservative assumption, since some time would elapse before commencement of maintenance and/or inspection operations) as input to the next calculational step, which models the distribution of nuclides throughout the cooling system.

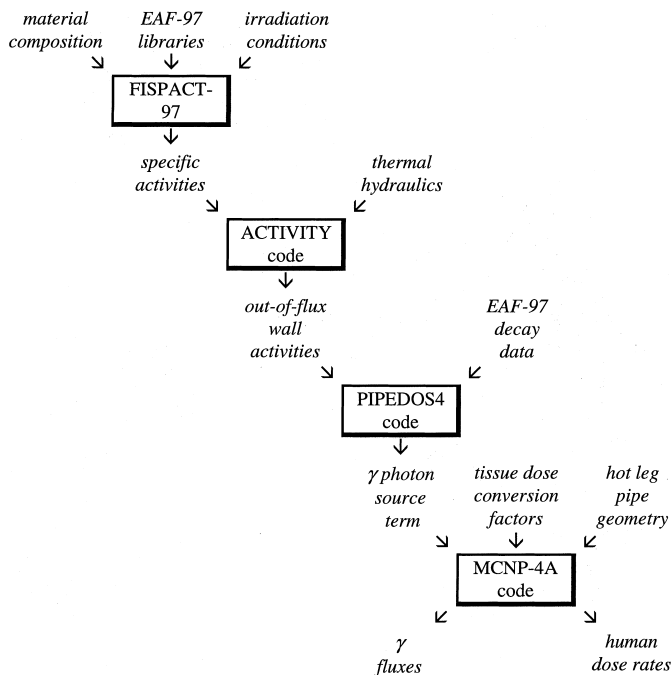


Fig. 2. Flow diagram showing the codes and data requirements for calculation of fluxes and dose rates.

Table 1
Starting composition (wt%) of alternative cooling circuit steels

Element	Austenitic steels		Martensitic steels	
	SS316	OPTSTAB	MANET-II	F-82H
C	0.1	0.07	0.11	0.09
Si	1.0	0.27	0.2	0.11
V	–	–	0.2	0.16
Cr	17	15.4	10.5	7.70
Mn	2.0	11.6	0.8	0.16
Fe	64.2	69.8	86.7	90.0
Co	0.09	0.001	0.005	0.005
Ni	12	0.005	0.6	0.02
Nb	0.01	0.00005	0.15	0.0001
Mo	2.5	0.002	0.6	0.003
Ta	0.05	0.5	–	0.02
W	–	2.05	–	1.95

2.2. ACP mobilisation, transport and deposition

The ACTIVITY code [7] was employed to calculate steady state concentrations of radionuclides in the coolant and on the inner surfaces of pipework both in and out of the blanket. For the present purposes of calculating γ fluxes and γ dose fields, only the wall deposits in out-of-flux regions are relevant. Input data required by ACTIVITY include the specific radionuclide activities, corrosion and dissolution rates for the structural material, mass transfer coefficients for the release and deposition of the soluble and insoluble particles and ions, and thermal hydraulic data for the cooling loop. Illustrative corrosion rates for both the austenitic and martensitic steels are based on previous LWR experience which were tabulated in Ref. [8]. Following the approach adopted in STARFIRE [9], the rate of release of crud particles was taken to be one third of the rate for the corrosion buildup. Corrosion and release rates were assumed to remain constant within and outside the blanket region. It is emphasised that the corrosion and crud release data employed are subject to large uncertainties since practically no measurements exist relevant to exposure under the conditions of ITER. Values of the cooling loop parameters used in the ACTIVITY code can be found in an earlier study [2].

2.3. Internal γ fluxes

The ACTIVITY code provides information on the activity concentrations of radionuclides deposited on the out-of-flux walls of the coolant circuit but gives no indication of the γ photon yields and energies needed for dose rate determination. To obtain the internal γ fluxes the code FISPACT-97 was utilised to process the photon emission data provided in the EAF-97 decay data library [6] into 24 discrete energy groups from which the ratio γ

$\text{m}^{-2} \text{s}^{-1}/\text{Bq m}^{-2}$ could be obtained for each nuclide. Activity concentrations in the wall deposits were then converted to an internal γ flux in the 24 group structure by means of the PIPEDOS4 code [2].

2.4. External γ fluxes and dose rates

In order to derive the photon fluxes and the corresponding tissue dose rates outside the pipe, the Monte Carlo photon transport code MCNP-4A [10] was employed. Dimensions for the hot-leg are based on loop parameters provided by Di Pace and Ceprega [11] with the simplification that the pipe is a straight pipe run carrying the coolant from the blanket ring manifolds to the heat exchanger. The inside radius of the pipe was taken as 28.73 mm, wall thickness as 1.73 mm and length 20 m. The relevant water coolant properties were: a temperature of 150°C, pressure 4 MPa and density 900 kg m^{-3} , while the steel density was assumed to be 8000 kg m^{-3} .

The photon-emitting deposit on the pipe wall was represented by a thin, uniformly distributed cylindrical surface source. The external γ flux was calculated at a position 1 m from the outside of the pipe halfway along the pipe section. MCNP-4A calculates partial fluxes in each energy interval and their summed totals after absorption and scattering through the pipe wall.

With the facility to incorporate energy group multipliers, the MCNP-4 code permits biological doses to be calculated together with the γ fluxes. The usual dose conversion factors were used to give a weighted average over body orientation and tissue types [9].

3. Results and discussion

Results from the five key calculational stages are summarised in Table 2. Only the total quantity for each

Table 2

Summary of results at each calculational stage and their relative ratio compared with SS316 steel

	Austenitic steels		Martensitic steels	
	SS316	OPTSTAB	MANET-II	F-82H
Specific activity (Bq kg ⁻¹)	9.76 × 10 ¹² (1)	1.99 × 10 ¹³ (2.04)	6.13 × 10 ¹² (0.63)	8.63 × 10 ¹² (0.88)
Surface activity deposited (Bq m ⁻²)	5.70 × 10 ⁹ (1)	7.14 × 10 ⁹ (1.25)	1.10 × 10 ¹¹ (19.3)	1.14 × 10 ¹¹ (20.0)
Internal γ flux (γ m ⁻² s ⁻¹)	4.29 × 10 ⁹ (1)	6.73 × 10 ⁹ (1.59)	4.72 × 10 ¹⁰ (11.73)	4.88 × 10 ⁹ (11.51)
External γ flux (γ m ⁻² s ⁻¹)	1.40 × 10 ⁸ (1)	2.97 × 10 ⁸ (2.12)	1.02 × 10 ⁹ (7.29)	9.81 × 10 ⁸ (7.01)
Dose rate (mSv h ⁻¹)	0.19 (1)	0.42 (2.21)	1.40 (7.37)	1.30 (6.84)

property is shown in this summary. Additionally, the ratio of each quantity, relative to the SS316 steel is given as an aid to inter-comparison. The salient points to note are:

1. Specific activities for all steels are similar, showing relatively small variation between highest and lowest values.
2. Total out-of-flux deposited surface activities for the martensitic steels are about 20 times larger than those for the austenitic materials, a difference largely attributable to the higher corrosion rates assumed for the martensitic steels.
3. The martensitic steels recover some benefit from having a lower proportion of penetrating photon emissions relative to austenitic steels, but they are nonetheless inferior in the final dose rate assessment.
4. Collective occupational doses would therefore be worse, if ITER were operated using unclad martensitic steel cooling pipes.
5. There are no clear ORE advantages in using low activation steel.

4. Conclusion

The mobilisation, transport and deposition of activated corrosion products in one FW/BL cooling loop of ITER has been modelled assuming the use of four alternative steel candidate materials. The calculated surface activity in out-of flux wall deposits is then used as the basis for assessing γ fluxes and γ dose rate fields around a representative hot-leg pipe in the same loop. Although not the ideal material in terms of induced material activation and γ photon emission strength, regarding ORE SS316 is the optimum candidate (of those examined) for use as the cooling loop material in ITER due to its greatly reduced corrosion rates relative to martensitic steels. The feasibility of cladding for martensitic steel cooling pipes requires further examination.

Acknowledgements

This work was jointly funded by the UK Department of Trade and Industry and by Euratom.

References

- [1] H.W. Bartels et al., Safety analysis data list-2 (SADL-2), Version 2.0.1., ITER JCT, Safety, Environment and Health division, Report No. S 81 97-05-04 W0.1, 5 May 1997.
- [2] C.B.A. Forty, P.J. Karditsas, Preliminary cooling circuit activation and ORE assessment for ITER, paper presented at 19th SOFT, Lisbon, September 16–20 1996.
- [3] J.-Ch. Sublet, Activation calculation modelling and operational scenario – sensitivity studies, UKAEA Report UKAEA/NID-4d/Sep1-1/3(94), 1994.
- [4] R.A. Forrest, J.-Ch. Sublet, FISPACT-97: User manual, UKAEA Report, UKAEA FUS 358, 1997.
- [5] J.-Ch. Sublet, J. Kopecky, R.A. Forrest, The European activation file: EAF-97 cross section library, UKAEA Report, UKAEA FUS 351, 1997.
- [6] R.A. Forrest, J.Ch. Sublet The European activation file: EAF-97 decay data library, UKAEA Report, UKAEA FUS 353, 1997.
- [7] K.R.Smith, C.B.A. Forty, Estimation of the radioactive content of the primary circuit of a water cooled fusion reactor and the annual liquid source term, UKAEA Report, AEA FUS 108, 1991.
- [8] J. Mustoe et al., Operator protection for a future commercial fusion power plant, paper presented at 19th SOFT, Lisbon, Sept.16–20, 1996.
- [9] C.C Baker et al., STARFIRE – A commercial tokamak fusion power plant study, ANL/FPP-80-1, Argonne National Laboratory, 1980, Appendix G.
- [10] J.F. Briesmeister (Ed.), MCNP – A general Monte Carlo code for neutron and photon transport, Los Alamos National Laboratory Report. LA-73396-M, Rev.2, 1986.
- [11] L.Di Pace, D.G. Ceprega, Evaluation of the activated corrosion products for the ITER heat transfer systems in support of NCSR-1, ENEA Report, ERG-FUS/TECN S+E TR 18/96, 1996.